Acquisition of Spontaneous Electrical Activity During Embryonic Development of Gonadotropin-Releasing Hormone-3 Neurons Located in the Terminal Nerve of Transgenic Zebrafish (*Danio rerio*)

Siddharth Ramakrishnan[1], **Wenjau Lee**[1,3], **Sammy Navarre**[2], **David J. Kozlowski**[2], and **Nancy L. Wayne**[1]

[1]Department of Physiology, David Geffen School of Medicine at University of California-Los Angeles, Los Angeles, California 90095

[2]Institute of Molecular Medicine and Genetics and Department of Cellular Biology and Anatomy, Medical College of Georgia, Augusta, Georgia 30912

Abstract

There are multiple populations of gonadotropin releasing hormone (GnRH) neurons that have distinct physiological and behavioral functions. Teleost fish have a population of GnRH3 neurons located in the terminal nerve (TN) associated with the olfactory bulb that is thought to play a neuromodulatory role in multiple physiological systems, including olfactory, visual, and reproductive. We used transgenic zebrafish in which the GnRH3 promoter drives expression of a green fluorescent protein to identify GnRH3 neurons during development in live embryos. Unlike with hypophysiotropic GnRH neurons of zebrafish, TN-GnRH3 neurons are of neural crest origin and are one of the first populations of GnRH neurons to develop in the early embryo. Using a combination of optical imaging and electrophysiology, we showed that during the first three days post-fertilization, TN-GnRH3 neurons increase in number, extend neural projections, move in association with tissue expansion, and acquire an adult-pattern of spontaneous action potential firing. Early during development, about half of the neurons were quiescent/non-firing. Later, at three days post-fertilization, there was an increase in the proportion of neurons showing action potential firing and an increase in the number of neurons that showed an adult-like tonic or beating pattern of action potential firing with a firing frequency similar to that seen in adult TN-GnRH3 neurons. This study represents the first neurophysiological investigation of developing GnRH neurons in live embryos -- an important advance in understanding their potential non-reproductive roles during embryogenesis.

Keywords

action potential; electrophysiology; embryo; teleost

Corresponding Author: Nancy L. Wayne, Department of Physiology, Room 231, Center for Health Sciences, David Geffen School of Medicine at University of California-Los Angeles Los Angeles, CA 90095. nwayne@mednet.ucla.edu; Tel: 310-794-1159; FAX: 310-206-5661.
[3]Current address: Department of Bioscience Technology, Chang Jung Christian University, Taiwan

INTRODUCTION

There are multiple populations of gonadotropin-releasing hormone (GnRH) neurons in all vertebrates investigated, and these are distinguished by their location in the central nervous system as well as particular patterns of GnRH gene expression. The most extensively studied population is hypophysiotropic neurons expressing GnRH1, which are located in the preoptic area and hypothalamus. These GnRH1 neurons regulate pituitary-gonadal functions and are the command cells for controlling reproductive development and fertility (Somoza et al., 2002; Okubo and Nagahama, 2008). In contrast, GnRH2 neurons are located in the midbrain tegmentum, and are thought to play a role integrating metabolic signals with reproductive function (Kauffman et al., 2005, 2006). Some teleost fishes have a third population of GnRH3 neurons located in the terminal nerve (TN) associated with the olfactory bulb. A definitive role for TN-GnRH3 neurons in physiology and/or behavior remains unclear. However, based on anatomical and physiological studies, these neurons are thought to play a neuromodulatory role in multiple systems, including olfactory, visual, and reproductive (Oka and Matsushima 1993; Yamamoto et al. 1997; Eisthen et al. 2000; Behrens and Wagner 2004; Ramakrishnan and Wayne, 2009).

In zebrafish, combined lineage tracing and GnRH mRNA/peptide histological analyses suggest that TN-GnRH3 neurons are of neural crest origin and hypophysiotropic GnRH3 neurons (aka, $^{(Trp7, Leu8)}$GnRH1 neurons) arise from the adenohypophyseal region of the developing anterior neural plate (Whitlock et al., 2003), challenging earlier and more recent work pointing to an olfactory-region or nasal-placode origin for hypophysiotropic GnRH neurons (Schwanzel-Fukuda and Pfaff, 1989; Wray et al., 1989; Whitlock, 2005; Abraham et al., 2009; Metz and Wray, 2010). Regardless of where GnRH neurons are born, specific populations of GnRH neurons develop patterns of electrical activity characteristic of their final locations in the adult (Oka, 2009). However, it is unclear when, where, or how these patterns of electrical activity are established following the birth any population of GnRH neurons.

We focused our attention on GnRH3 neurons located in the TN because of their relatively easy accessibility for electrophysiological recordings in the zebrafish embryo. Further, the electrophysiology of TN-GnRH3 neurons in the adults of other species of fish is well characterized (Oka and Matsushima, 1993; Wayne et al., 2005; Nakane and Oka, 2010), which is important for understanding maturation of their electrical activity. Current evidence suggests that significant cellular changes occur in the TN population during the first several days post-fertilization in zebrafish. Studies using *in situ* hybridization (Gopinath et al., 2004) and transgenic expression of GnRH3:GFP transgenes in GnRH neurons in living embryos (Palevitch et al., 2007; Abraham et al., 2008) show that developing TN-GnRH3 neurons are first detected around 24 h post-fertilization (hpf) adjacent to the developing olfactory organ, with progressive increases in cell number between 30 and 48 hpf. Axon projections were first noted at about 26 hpf, which is within 2 h of GFP expression in the soma, and become more extensive over the next 3-4 days of embryogenesis (Abraham et al., 2008). We hypothesized that in conjunction with these morphological changes, there are neurophysiological changes taking place in TN-GnRH3 neurons during embryonic development, which may presage their differentiated functions in the adult.

In the present study, we investigated the neurophysiological development of TN-GnRH3 neurons in stable lines of transgenic zebrafish in which the GnRH3 promoter drives expression of an Emerald Green Fluorescent Protein (EMD). Because zebrafish embryos are transparent, this transgenic model system provides us with the unique opportunity to identify GnRH3 neurons *in vivo* for neurophysiological recording. Further, TN-GnRH3 neurons are located within tens of micrometers to the surface of the embryo brain and the soma is

relatively large (> 15 μm), making them an accessible target for electrophysiology. In coordination with morphological changes in the TN-GnRH3 population, we investigated acquisition of spontaneous action potential firing during embryogenesis.

MATERIALS AND METHODS

Animals

The *brass* mutant-line of zebrafish was used to generate the transgenic fish. At both UCLA and Medical College of Georgia, animals were maintained in zebrafish aquarium systems on a 14L:10D photoperiod at 28 °C. Fish were fed twice daily with flake food and live brine shrimp. All procedures were carried out in accordance with and approved by the Animal Care and Use Committees of UCLA and Medical College of Georgia.

Generation of constructs and transgenic fish

The GnRH3:EMD transgene was constructed as follows: A 6.11 kb genomic DNA fragment containing the zebrafish GnRH3 promoter, signal sequence, and open reading frame (ORF) was amplified from BAC clone CH211-207N2 (5′-TTTTGGCTCGAGACTTCTAC; 5′-ATACCCGCGGTAACCGGGAAGCCAACC GTATG; gift from Dr. Arnaud Lacoste) and subcloned into pCR-XL-TOPO (Invitrogen, Carlsbad, CA). An XhoI – SacII fragment was then subcloned into the expression vector pBI2-EGFP (Clontech, Mountain View, CA), where EGFP was replaced by Emerald (EMD) sequence (Invitrogen). This clone was further modified to delete the GnRH3 peptide open reading frame using primers (5′-GAGGTCAGTCTTTGCATGGTGAGCAAGG; 5′-CCTTGCTCACCATGCAAAGACTGACCTC) and the QuikChange procedure (Stratagene, La Jolla, CA). The final GnRH3:EMD transgene contained ~6.0 kb GnRH3 promoter sequence, and the GnRH3 signal sequence fused in frame EMD open reading frame. All clones and constructs were verified by sequencing of both DNA strands (UCLA Sequencing and Genotyping Core facility).

To generate transient and germline transgenic embryos and zebrafish, 50 pg (50 ng/μl) of linear or circular plasmid transgene DNA was microinjected into the yolk of 1-4 cell stage zebrafish embryos. Transient expression of the transgene was confirmed the next day by fluorescence microscopy or RT-PCR of RNA prepared from embryos. Microinjected embryos were raised to sexual maturity and germline transgenic zebrafish were identified by random-pair mating and monitoring of transgene expression (EMD fluorescence or RT-PCR) in the F1 and subsequent generations.

Immunohistochemistry

Three-day post-fertilization embryos were fixed for 4 hours at room temperature in 4% paraformaldhyde with 0.2% picric acid in phosphate buffered saline (PBS) (0.26% sodium phosphate monobasic; 1.15% sodium phosphate anhydrous dibasic; 0.9% sodium chloride; pH 7.2). Fixed embryos were washed and stored in PBS in the dark at 4 °C. Prior to processing, embryos were cryoprotected in 20% sucrose solution (in PBS) for 24 h at 4 °C in the dark. Preparations were then embedded in TissueTek (VWR Int., Westchester, PA) medium, frozen on dry ice, and sectioned (10 μm) using a cryostat. Sections were rinsed in 0.3% Tween solution in PBS and blocked for 2 h at room temperature in the dark with a solution of 0.3% Tween and 2% goat serum (in PBS). Following blocking, sections were washed and incubated overnight at 4 °C with the primary antibody (LRH13, mouse anti-GnRH, 1:3000) diluted in the blocking solution. After washing with 0.3% Tween in PBS, sections were incubated in the secondary antibody (Alexa Fluor 594 anti-mouse, 1:100; Invitrogen, Carlsbad, CA). Sections were rinsed in PBS prior to mounting on slides with the Vectashield mounting medium (Vector Labs, Burlingame, CA).

Histological sections were observed using a confocal imaging system (with Fluoview imaging software) attached to an Olympus microscope (Olympus America Inc, Center Valley, PA). Images were taken using a 40x objective. EMD fluorescence was observed using an Argon laser (488 nm) with an emission barrier filter of 510 nm. Alexa Fluor 594 (secondary antibody staining) was visualized using a HeNe laser (543nm) with an emission filter of 560-600 nm. For each optical section of the slices along the z-plane the EMD and Alexa Fluor emissions were recorded separately. Control embryos were processed the same as the experimental animals with the exception of incubation without the primary antibody. Control brain sections were imaged using the same excitation and emission wavelengths and laser intensity as experimental animals within the same cohort of embryos. NIH Image (http://rsb.info.nih.gov/) and Adobe Photoshop (Adobe Systems Inc, San Jose, CA) were used to prepare the images for viewing. Control and experimental images were adjusted equally (gamma correction/image levels) to enhance picture quality.

Confocal microscopy of living embryos

Embryos (1-2 days post-fertilization, dpf) were manually dechorionated, embedded in a drop of 0.8% agarose (Fisher Scientific, Pittsburgh, PA) and oriented using blunt forceps. Once the agarose solidified, a drop of fish saline was added to keep the agarose moist. Embryos were then viewed under an Olympus confocal microscope and imaged using the Fluoview imaging system (Olympus America Inc., Center Valley, PA). Images were taken using a water immersion 40x objective. EMD fluorescence was observed using an Argon laser (488 nm) with an emission barrier filter of 510 nm. Optical sections were made every 0.5 μm along the z-axis from the dorsal to the ventral side of the embryo. In some cases, final images were achieved through projections of the z stack. Time-lapse images were acquired by scanning the embryos approximately every hour. Once the z stacks were obtained for each time-point, these were then compiled together to form time-lapse videos using Windows Movie Maker (Microsoft Inc., Redmond, WA). Individual images (either each plane in a z stack or projections of the z stack) were processed using the Fluoview imaging software, NIH Image, and Adobe Photoshop.

Electrophysiology

Embryonic zebrafish (2-3 dpf) were anesthetized by immersion in MS-222 (150 mg/l). They were glued ventral-side up to a glass coverslip at the bottom of a flow-through recording chamber (P1; Warner Instrument Corp., Hamden, CT). Temperature in the recording chamber was maintained at 21-22 °C throughout the experiments. Following transfer to the recording chamber, the developing tissue covering the ventral side of the brain from the optic nerves to the olfactory bulbs was scraped carefully away, allowing access to the cells for electrophysiology. Details of the procedure for both whole-cell current clamp electrophysiology and loose-patch electrophysiology have been previously described (Wayne et al. 2005). All chemicals were bought from Sigma-Aldrich, Inc. (St. Louis, MO, USA). Aerated solution was continuously perfused through the recording chamber at a rate of approximately 200 μl/min, and contained in mM: 134 NaCl; 2.9 KCl; 2.1 $CaCl_2$; 1.2 $MgCl_2$; 10 Hepes. Osmolarity was adjusted to 290 mOsm with glucose, and pH was adjusted to 7.8 with NaOH. Tubocurarine (50 μM) was added to the external solution in order to prevent movement and muscle contractions during recording. The internal solution for the whole-cell patch pipette (Itri et al. 2004) contained in mM: 112.5 K-gluconate; 4 NaCl; 17.5 KCl; 0.5 CaCl2; 1 MgCl2; 5 MgATP; 1 EGTA; 10 Hepes; 1 GTP; 0.1 leupeptin; 10 phosphocreatine. Osmolarity was adjusted to 290 mOsm by titrating the final volume of water, and pH was adjusted to 7.2 with KOH. The solution for the loose-patch pipette (Nunemaker et al., 2003) contained 150 mM NaCl, 3.5 mM KCl, 2.5 mM CaCl2, 1.3 mM MgCl2, 10 mM Hepes, and 10 mM glucose. Osmolarity was adjusted to 290 mOsm, and pH was adjusted to 7.4 with NaOH.

TN-GnRH3 neurons expressing EMD were visualized under an upright microscope (BX50W, Olympus, Melville, NY, USA) using a combination of infrared differential-contrast (IR-DIC) optics and an IR-camera (OL-1500, Olympus), and in the presence of both UV- and brightfield illumination. Electrical activity was monitored either with a whole-cell patch electrode (resistance between 7–10 M Ohms) or a loose-patch electrode (resistance ~ 6 M Ohms) pulled from borosilicate glass (1.5mm diameter, WPI, Sarasota, FL; P87, Sutter Instruments, Novato, CA, USA). Whole-cell recordings of membrane potential (Vm) and action potentials were obtained using an Axopatch 200B amplifier (Axon Instruments, Foster City, CA, USA) in current-clamp mode, and digitized with an ITC-18 computer interface (Instrutech Corp., Port Washington, NY, USA). Recordings were monitored online using both AxoGraph software (Axon Instruments, Foster City, CA, USA) and PowerLab data acquisition and analysis instrumentation and software (ADInstruments Inc., Colorado Springs, CO, USA), and stored off-line for subsequent AxoGraph data analysis of interspike Vm, spike frequency, and action potential amplitude. Data were collected if series resistance was < 35 M Ohms and if interspike Vm was at least −40 mV. Recordings from EMD-expressing neurons were positively identified by visualizing diffusion of EMD into the tip of the recording electrode (Fig. 1H, I).

For loose-patch recordings, a low-resistance seal (~30 M Ohms) was obtained following release from positive pressure. Data (spike frequency) were collected once the baseline recording stabilized (usually within 5 min from seal formation). Recordings from EMD-expressing neurons were positively identified at the end of each experiment by visualizing fluorescence from recorded neurons that were either sucked into or attached to the tip of the electrode. The average time of recording on day 2 was 52 hpf, and on day 3 was 76 hpf.

Data analysis

Mann-Whitney U test was used to compare characteristics of TN-GnRH3 neuron electrical activity from 2 dpf and 3 dpf embryos: frequency of action currents during tonic firing and during bursting; burst duration; and, inter-burst interval. The three activity patterns (silent, bursting, and tonic action potential firing) were defined as follows. Neurons that showed a firing frequency < 0.015 Hz during the recording period were labeled as 'silent'. Neurons that showed a period of action potential firing of at least 1.5 Hz surrounded by period of no action potential firing were labeled as 'bursting'. The average inter-burst interval was 38 sec at 2dpf and 10 sec at 3 dpf (Fig. 4C). Neurons that showed continuous action potential firing throughout the recording period with a frequency of 0.015 Hz or greater were labeled as 'tonic firing'. Fisher's Exact Test compared the proportion of neurons that showed action currents from 2 dpf and 3 dpf embryos. Data between age groups were considered significantly different if $P < 0.05$.

RESULTS

Transgenic zebrafish and expression of the GnRH3:EMD transgene

To visualize GnRH neurons *in vivo* and during embryogenesis, transgenic zebrafish expressing EMD under control of the GnRH3 promoter were generated. To verify that EMD expressing cells are GnRH neurons, immunohistochemical verification of expression of the transgene was performed on n=6 GnRH3:EMD embryos ages 2-3 dpf (Fig. 1C-E). All EMD-expressing neurons (n = 21 cells) in TN colocalized with immunodetectable GnRH peptide, and 90% of immunoreactive-GnRH neurons (21 out of 23 cells) expressed detectable levels of EMD. Control brain sections incubated with secondary antibody (no primary antibody) showed no non-specific fluorescence of neural structures (Fig. 1F, G). Therefore, every EMD-expressing neuron in the olfactory region of the embryo was verified to be a GnRH3 neuron.

Fig. 1A, B shows confocal images (projection of z-stack) of EMD expression in bilateral clusters of neurons located in the olfactory region of a GnRH3:EMD transgenic embryo at 27 hpf and 47 hpf. Based on both confocal imaging of live embryos and immunohistological analysis of fixed embryos, there was a consistent increase in the number of TN-GnRH3:EMD neurons and extent of axon outgrowth into the region of the olfactory bulbs between 27 and 47 hpf (Fig. 1A, B; Supplement 1). Each bilateral cluster of TN-GnRH3:EMD neurons contained approximately 6 cells (at 48 hpf) to 9 cells (at 72 hpf). During embryonic morphogenesis (between 48 – 70 hpf), the bilateral clusters of TN-GnRH3:EMD neurons became more anteriorly displaced relative to its initial position at the start of imaging (Fig. 2). This displacement did not appear to be cellular migration; rather, time-lapse confocal microscopic imaging revealed that the bilateral clusters of neurons appeared to passively change position, along with the nares, as the result of tissue expansion.

Electrophysiology of GnRH3:EMD neurons at 2 dpf and 3 dpf

A total of n=79 GnRH3:EMD neurons from the olfactory region were recorded from 46 embryos. Based on the heart beating and electrophysiological recordings, the embryos remained viable for at least 3 h during the recording experiments. We successfully recorded from n=3 TN-GnRH3:EMD neurons from 3 different embryos on 2 dpf, and n=2 neurons from 2 different embryos on 3 dpf (Fig. 3). Interspike Vm was -64.7 ± 4.3 mV at 2 dpf, and -45.8 ± 3.7 at 3 dpf. This level of relative depolarization at 3 dpf is similar to that reported for adult TN-GnRH3 neurons (Oka and Matsushima, 1993; Wayne et al., 2005), and suggests neuronal maturation during embryonic development. The 2 dpf neurons showed either infrequent action potentials or short bursts of action potentials; whereas both 3 dpf neurons showed a beating or tonic pattern of spontaneous action potential firing (1.65 ± 0.3 Hz; 42 ± 17 mV amplitude), similar to that reported for adult TN-GnRH3 neurons but with a lower spike amplitude by about half.

Compared to adult TN-GnRH3 neurons (Wayne et al., 2005, 2007), embryonic TN-GnRH3 neurons are more fragile and easily damaged when attempting whole-cell patch recording, so we turned to a single-cell extracellular recording technique, loose-patch recording, that has been successfully employed for detecting action potentials/action currents from adult GnRH neurons (Nunemaker et al., 2003; Wayne et al., 2005; Nakane and Oka, 2010). Similar to the whole-cell patch recordings, Fig. 4 shows that there were developmental changes in electrical activity of TN-GnRH3:EMD neurons between 2 dpf and 3 dpf. The duration of recordings averaged 9.84 ± 0.95 min (range: 2 to 28 min). Within the period of recording, 48% of 2-dpf neurons showed few to no action currents (frequency < 0.015 Hz), decreasing to 19% of the population showing few to no action currents at 3 dpf ($P < 0.05$). At 2 dpf, 31% of total neurons showed a bursting pattern of action currents, and 21% showed a tonic pattern of activity. At 3 dpf, 31% of total neurons showed a bursting pattern of action currents – very similar to what was seen at 2 dpf. However, the percent of neurons showing a tonic pattern of action currents increased to 50% of total at 3 dpf (Fig. 4A). Between 2 dpf and 3 dpf, there was a significant increase in the frequency of action currents for those neurons showing a tonic pattern of activity ($P<0.001$), increase in frequency of action currents within each burst for those neurons showing a bursting pattern of activity ($P<0.05$), decrease in burst duration ($P<0.05$) and decrease in inter-burst interval ($P< 0.025$) (Fig. 4F-I).

DISCUSSION

The present study supports and extends work using both transgenic and non-transgenic zebrafish, that demonstrate a developmental increase in the number of TN-GnRH3 neurons during the first days of embryogenesis (Gopinath et al., 2004; Palevitch et al., 2007; Abraham et al., 2008). Further, we have shown for the first time developmental changes in

electrical activity of any population of GnRH neurons in the living embryo, and these changes correspond to the patterns of electrical activity characteristic of their differentiated fate. We focused on the terminal nerve population of GnRH3 neurons because they develop early in zebrafish embryos (Gopinath et al. 2003; Palevitch et al., 2007; Abraham et al., 2008), are relatively easy to access for electrophysiological recordings in the live embryo, and the electrophysiology of these neurons in adults of other species of fish is well characterized (Oka and Matsushima, 1993; Wayne et al., 2005; Nakane and Oka, 2010). Our findings show that between 2 and 3 dpf, the TN-GnRH3:EMD neurons acquire an adult-like pattern of spontaneous action potential firing (Oka and Matsushima, 1993; Wayne et al., 2005). Whole-cell recordings demonstrated that within this 24 hr period, GnRH3:EMD neurons became more depolarized and acquired a tonic pattern of action potential firing. The interspike Vm and frequency of action potential firing at 3 dpf was similar to what has been shown in adult TN-GnRH3 neurons from adult dwarf gourami and medaka fish (Oka and Matsushima, 1993; Wayne et al., 2005). Loose-patch extracellular recording supported the developmental increase in the proportion of TN-GnRH3 neurons that showed a tonic pattern of action potential firing. This acquisition of an adult-like pattern of electrical activity occurred during the embryonic movement of the GnRH3 neurons towards their final location in the terminal nerve. It was not technically feasible to record from older zebrafish TN-GnRH3 neurons, so we cannot compare patterns of electrical activity at larval or adult stages. Unlike with dwarf gourami and medaka, the zebrafish GnRH3 neurons become inaccessible for recording because they become ensheathed within the terminal nerve bundle towards the mid-to-end of 3 dpf (data not shown; this was apparent during recordings when we could no longer access the neurons). It is highly likely that adult zebrafish TN-GnRH3 neurons show similar electrophysiological characteristics as reported in dwarf gourami and medaka.

Although these studies do not address directly the physiological significance of GnRH3 neurons acquiring an adult-like pattern of electrical activity at 3 dpf, previous studies using embryonic rodent model systems and cell cultures have supported the hypothesis that there is a functional relationship between neuronal activity and migration/fiber extension of GnRH neurons. In all of this work, low electrical activity promoted GnRH neuron migration, whereas high electrical activity suppressed migration. Indeed, treating embryonic olfactory placode-derived GnRH neurons with TTX to block action potential firing stimulated migratory activity (Fueshko et al., 1998). On the other hand, treating animals or explants with GABA$_A$-receptor agonists or activating GAD-67 prematurely arrested migration and decreased GnRH neuronal projections (Fueshko et al., 1998; Bless et al., 2000; Heger et al., 2003). [It should be noted that in both hypothalamic and terminal-nerve GnRH neurons, activating GABA$_A$-receptors is excitatory (Moenter and Defazio, 2005; Nakane and Oka, 2010).] Furthermore, altering electrical activity in an immortalized GnRH cell line (GN11) affected cell migration. GN11 cells normally display low electrical activity and high chemomigratory activity. However, membrane depolarization, which normally accompanies neuronal maturation, decreased migratory activity in GN11 cells (Pimpinelli et al., 2003). In the present study, the period of electrical quiescence could correspond to migration of GnRH3 neurons from the dorsal neural tube to their location near the olfactory epithelium. Once at the olfactory epithelium between 2 – 3 dpf, the GnRH3 neurons increase their electrical activity - which could provide a stop signal for migration. At this point, the bilateral clusters of GnRH3 neurons passively move with morphogenetic tissue movements.

It is well documented that action-potential firing stimulates neuropeptide secretion (Dyball and Koizumi, 1969; Renaud and Bourque, 1991; Wayne, 1995), including from GnRH neurons (Krsmanovic et al., 2009). Assuming that GnRH peptide being expressed in the zebrafish embryo is packaged into secretory vesicles that are then docked at the plasma membrane, it is likely that early acquisition of action potential firing would stimulate GnRH

secretion – and perhaps mediate the effects of electrical activity on neuron development. Importantly, antisense morpholino knockdown of GnRH expression interfered with normal brain and eye formation, as well as disrupted development of GnRH-neuron projections and localization of their somas in the zebrafish embryo (Wu et al., 2006; Abraham et al., 2008). Further, GnRH neurons in the olfactory region were shown to project widely in the developing brain, and appeared to innervate the eye (Abraham et al., 2008). Recent work using an *in vitro* olfactory nerve bundle preparation (containing migrating GnRH1 neurons) from embryonic chick supports the hypothesis that GnRH secretion plays an important role in regulating the development of GnRH neurons (Kanaho et al., 2009). Specifically, it was shown that a GnRH antagonist inhibited GnRH neurite extension, the number of migrating GnRH1 neurons, and the distance of migration. All of these effects were reversed with simultaneous treatment with cGnRH1. Together, this growing body of work suggests that GnRH secretion – which is controlled by action potential firing -- is playing an important role in the developing embryo, apart from its better-known role in controlling reproductive functions. Our present study shows that GnRH neurons become neurophysiologically mature at a very young age, further implicating a physiological role for these neurons in the developing embryo.

Supplementary Material

Refer to Web version on PubMed Central for supplementary material.

Acknowledgments

REFERENCES

Abraham E, Palevitch O, Ijiri S, Du SJ, Gothilf Y, Zohar Y. Early development of forebrain gonadotrophin-releasing hormone (GnRH) neurones and the role of GnRH as an autocrine migration factor. J. Neuroendocrinol. 2008; 20:394–405. [PubMed: 18208553]

Abraham E, Palevitch O, Gothilf Y, Zohar Y. The zebrafish as a model system for forebrain GnRH neuronal development. Gen. Comp. Endocrinol. 2009; 164:151–160. [PubMed: 19523393]

Behrens U, Wagner HJ. Terminal nerve and vision. Microsc. Res. Tech. 2004; 65:25–32. [PubMed: 15570588]

Bless EP, Westaway WA, Schwarting GA, Tobet SA. Effects of gamma-aminobutyric acid(A) receptor manipulation on migrating gonadotropin-releasing hormone neurons through the entire migratory route *in vivo* and *in vitro*. Endocrinology. 2000; 141:1254–1262. [PubMed: 10698203]

Dyball RE, Koizumi K. Electrical activity in the supraoptic and paraventricular nuclei associated with neurohypophysial hormone release. J. Physiol. 1969; 201:711–722. [PubMed: 5767890]

Eisthen HL, Delay RJ, Wirsig-Wiechmann CR, Dionne VE. Neuromodulatory effects of gonadotropin releasing hormone on olfactory receptor neurons. J. Neurosci. 2000; 20:3947–3955. [PubMed: 10818129]

Fueshko SM, Key S, Wray S. GABA inhibits migration of luteinizing hormone-releasing hormone neurons in embryonic olfactory explants. J. Neurosci. 1998; 18:2560–2569. [PubMed: 9502815]

Gopinath A, Tseng LA, Whitlock KE. Temporal and spatial expression of gonadotropin releasing hormone (GnRH) in the brain of developing zebrafish (*Danio rerio*). Gene Expr .Patterns. 2004; 4:65–70. [PubMed: 14678830]

Heger S, Seney M, Bless E, Schwarting GA, Bilger M, Mungenast A, Ojeda SR, Tobet SA. Overexpression of glutamic acid decarboxylase-67 (GAD-67) in gonadotropin-releasing hormone neurons disrupts migratory fate and female reproductive function in mice. Endocrinology. 2003; 144:2566–2579. [PubMed: 12746320]

Itri J, Michel S, Waschek JA, Colwell CS. Circadian rhythm in inhibitory synaptic transmission in the mouse suprachiasmatic nucleus. J. Neurophysiol. 2004; 92:311–319. [PubMed: 14973316]

Kanaho YI, Enomoto M, Endo D, Maehiro S, Park MK, Murakami S. Neurotrophic effect of gonadotropin-releasing hormone on neurite extension and neuronal migration of embryonic gonadotropin-releasing hormone neurons in chick olfactory nerve bundle culture. J. Neurosci. Res. 2009; 87:2237–2244. [PubMed: 19301422]

Kauffman AS, Wills A, Millar RP, Rissman EF. Evidence that the type-2 gonadotrophin-releasing hormone (GnRH) receptor mediates the behavioural effects of GnRH-II on feeding and reproduction in musk shrews. J. Neuroendocrinol. 2005; 17:489–497. [PubMed: 16011485]

Kauffman AS, Bojkowska K, Wills A, Rissman EF. Gonadotropin-releasing hormone-II messenger ribonucleic acid and protein content in the mammalian brain are modulated by food intake. Endocrinology. 2006; 147:5069–5077. [PubMed: 16873537]

Krsmanovic LZ, Hu L, Leung PK, Feng H, Catt KJ. The hypothalamic GnRH pulse generator: multiple regulatory mechanisms. Trends Endocrinol. Metab. 2009; 20:402–408. [PubMed: 19740674]

Metz H, Wray S. Use of mutant mouse lines to investigate origin of gonadotropin-releasing hormone-1 neurons: lineage independent of the adenohypophysis. Endocrinology. 2010; 151:766–773. [PubMed: 20008041]

Moenter SM, DeFazio RA. Endogenous GABA can excite GnRH neurons. Endocrinology. 2005; 146:5374–5379. [PubMed: 16123153]

Nakane R, Oka Y. Excitatory action of GABA in the terminal nerve gonadotropin-releasing hormone neurons. J. Neurophysiol. 2010 doi:10.1152/jn.00910.2009.

Nunemaker CS, DeFazio RA, Moenter SM. A targeted extracellular approach for recording long-term firing patterns of excitable cells: a practical guide. Biol. Proced. Online. 2003; 5:53–62. [PubMed: 12734556]

Oka Y, Matsushima T. Gonadotropin-releasing hormone (GnRH)-immunoreactive terminal nerve cells have intrinsic rhythmicity and project widely in the brain. J. Neurosci. 1993; 13:2161–2176. [PubMed: 7683049]

Oka Y. Three types of gonadotrophin-releasing hormone neurones and steroid-sensitive sexually dimorphic kisspeptin neurones in teleosts. J. Neuroendocrinol. 2009; 21:334–338. [PubMed: 19210296]

Okubo K, Nagahama Y. Structural and functional evolution of gonadotropin-releasing hormone in vertebrates. Acta Physiol. (Oxf.). 2008; 193:3–15. [PubMed: 18284378]

Palevitch O, Kight K, Abraham E, Wray S, Zohar Y, Gothilf Y. Ontogeny of the GnRH systems in zebrafish brain: in situ hybridization and promoter-reporter expression analyses in intact animals. Cell Tissue Res. 2007; 327:313–322. [PubMed: 17036230]

Pimpinelli F, Redaelli E, Restano-Cassulini R, Curia G, Giacobini P, Cariboni A, Wanke E, Bondiolotti GP, Piva F, Maggi R. Depolarization differentially affects the secretory and migratory properties of two cell lines of immortalized luteinizing hormone-releasing hormone (LHRH) neurons. Eur. J. Neurosci. 2003; 18:1410–1418. [PubMed: 14511321]

Ramakrishnan S, Wayne NL. Social cues from conspecifics alter electrical activity of gonadotropin-releasing hormone neurons in the terminal nerve via visual signals. Am. J. Physiol. Regul. Integr. Comp. Physiol. 2009; 297:R135–R141. [PubMed: 19420290]

Renaud LP, Bourque CW. Neurophysiology and neuropharmacology of hypothalamic magnocellular neurons secreting vasopressin and oxytocin. Prog. Neurobiol. 1991; 36:131–169. [PubMed: 1998074]

Schwanzel-Fukuda M, Pfaff DW. Origin of luteinizing hormone-releasing hormone neurons. Nature. 1989; 338:161–164. [PubMed: 2645530]

Somoza GM, Miranda LA, Strobl-Mazzulla P, Guilgur LG. Gonadotropin-releasing hormone (GnRH): from fish to mammalian brains. Cell. Mol. Neurobiol. 2002; 22:589–609. [PubMed: 12838906]

Wayne NL. The neuroendocrine bag cells of Aplysia: a model system for neural control of hormone secretion. J. Endocrinol. 1995; 147:1–4. [PubMed: 7490521]

Wayne NL, Kuwahara K, Aida K, Nagahama Y, Okubo K. Whole-cell electrophysiology of gonadotropin releasing hormone (GnRH) neurons that express green fluorescent protein (GFP) in the terminal nerve of transgenic medaka (*Oryzias latipes*). Biol. Reprod. 2005; 73:1228–1234. [PubMed: 16107608]

Wayne NL, Kuwahara K. Beta-endorphin alters electrical activity of gonadotropin releasing hormone neurons located in the terminal nerve of the teleost medaka (*Oryzias latipes*). Gen. Comp. Endocrinol. 2007; 150:41–47. [PubMed: 16919275]

Whitlock KE, Wolf CD, Boyce ML. Gonadotropin-releasing hormone (GnRH) cells arise from cranial neural crest and adenohypophyseal regions of the neural plate in the zebrafish, *Danio rerio*. Dev. Biol. 2003; 257:140–152. [PubMed: 12710963]

Whitlock KE. Origin and development of GnRH neurons. Trends Endocrinol. Metab. 2005; 16:145–151. [PubMed: 15860410]

Wray S, Grant P, Gainer H. Evidence that cells expressing luteinizing hormone-releasing hormone mRNA in the mouse are derived from progenitor cells in the olfactory placode. Proc. Natl. Acad. Sci. U.S.A. 1989; 86:8132–8136. [PubMed: 2682637]

Wu S, Page L, Sherwood NM. A role for GnRH in early brain regionalization and eye development in zebrafish. Mol. Cell. Endocrinol. 2006; 257-258:47–64. [PubMed: 16934393]

Yamamoto N, Oka Y, Kawashima S. Lesions of gonadotropin-releasing hormone-immunoreactive terminal nerve cells: effects on the reproductive behavior of male dwarf gouramis. Neuroendocrinology. 1997; 65:403–412. [PubMed: 9208402]
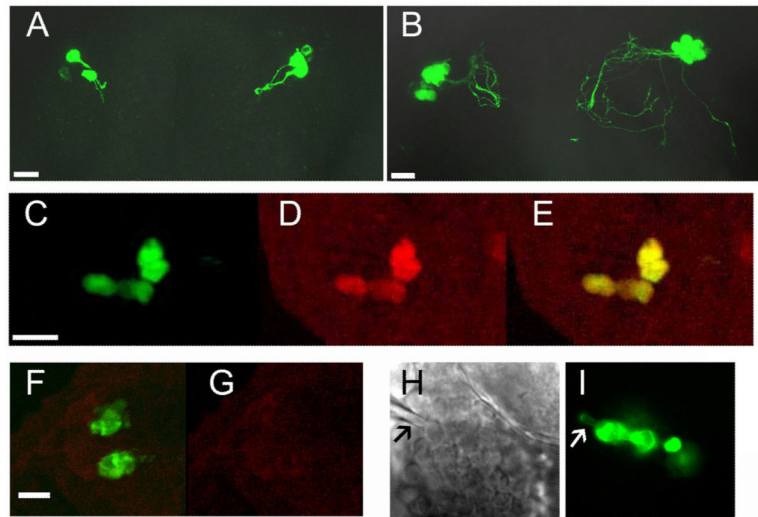
Figure 1.
Images of GnRH3:EMD neurons in zebrafish embryos. *A, B*: Confocal images of
GnRH:EMD neurons in the olfactory region of live embryos. *A:* 27 hpf; *B:* 47 hpf (same
embryo). Scale bar is 20 μm. *C-E*: Immunohistochemical (IHC) verification that EMD-
expressing neurons in the olfactory region contain immunoreactive (ir) GnRH peptide. *C:*
EMD fluorescence; *D:* irGnRH peptide; E: merged images of EMD and irGnRH. Scale bar
is 50 μm. *F, G:* IHC control tissue in the absence of primary anti-GnRH antibody showing
specificity of red fluorescence (i.e., irGnRH peptide). *F:* GFP fluorescence; *G:* IHC
experiment in the absence of primary antibody. Scale bar is 10 μm. *H, I:* Verification that
neurons targeted for whole-cell electrophysiology are EMD-containing neurons. *H:*
Brightfield image of the intact brain in the olfactory region in the live embryo. *I:* EMD
image (same field of view as in H) showing a string of GnRH3:EMD neurons in the
olfactory region. EMD diffuses into the tip of the electrode (marked by arrow) during
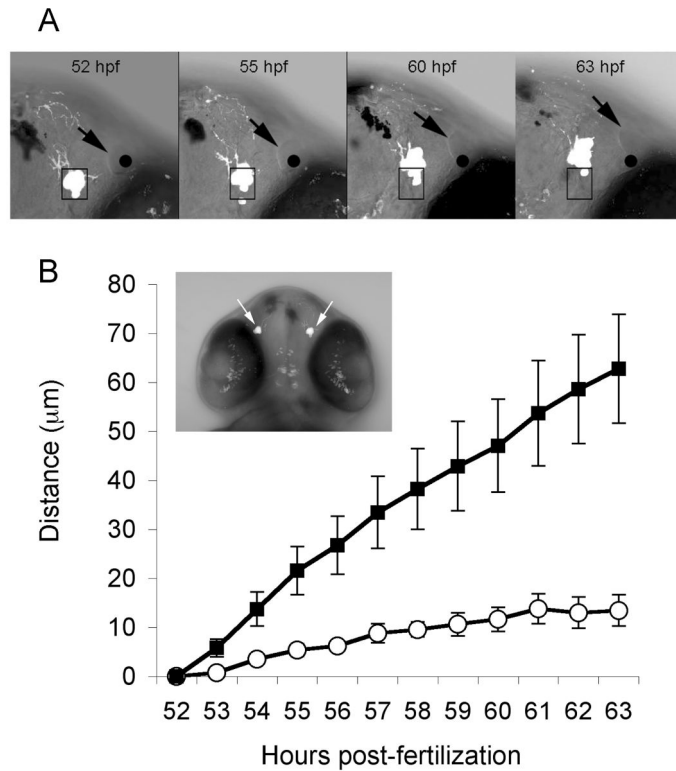whole-cell recording (I).

Figure 2.
Displacement of GnRH3:EMD neurons in the live, intact embryo at 2 dpf. *A:* Merged fluorescence and brightfield confocal images (single optical slice) from the same field of view at different times during development. Shown are representative images of the right upper quadrant of an embryo head over time (same embryo as shown in panel *B* insert). A box was positioned around the right GnRH3:EMD neuron cluster and a black dot was positioned at the center of the opening of the right nare at 52 hpf. The position of the box and dot were kept constant, relative to the field of view in subsequent images, revealing displacement of the GnRH3:EMD cluster and nare over this time period. Black arrows point to the edge of the opening of the nare. *B:* Displacement of GnRH3:EMD clusters from 52 – 63 hpf (mean ± SEM; four clusters from two embryos). Y-axis refers to distance moved relative to the location of clusters at 52 hpf. Displacement in an anterior direction is shown by the black squares; displacement in a lateral direction is shown by the open circles. The insert shows the entire head of the embryo (projection of the z stack) at 52 hpf; arrows point to the bilateral TN-GnRH3:EMD neuron clusters.
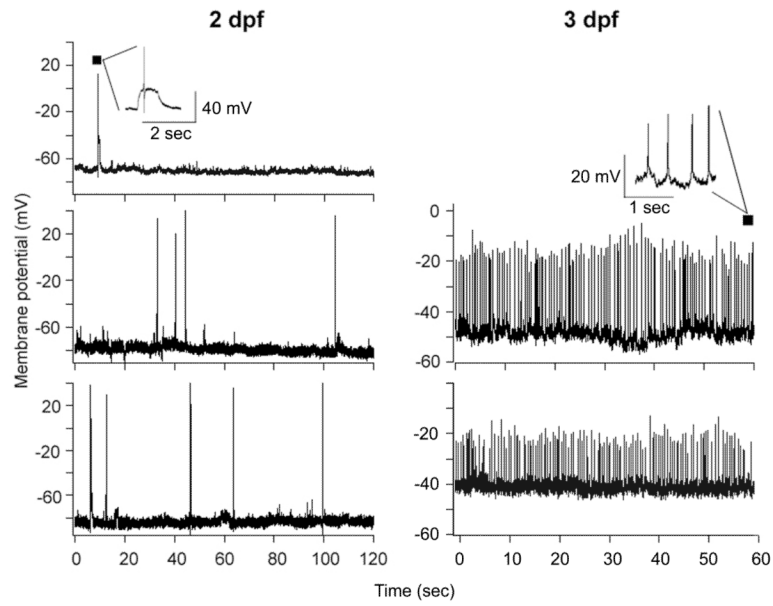
Figure 3.
Whole-cell current clamp recordings from TN-GnRH3:EMD neurons from 2 and 3 dpf transgenic embryos. Shown are excerpts from longer recording sessions. Inserts from the top traces of 2 and 3 dpf embryos show representative details from the recordings. Note that the x and y axes are different between 2 and 3 dpf.
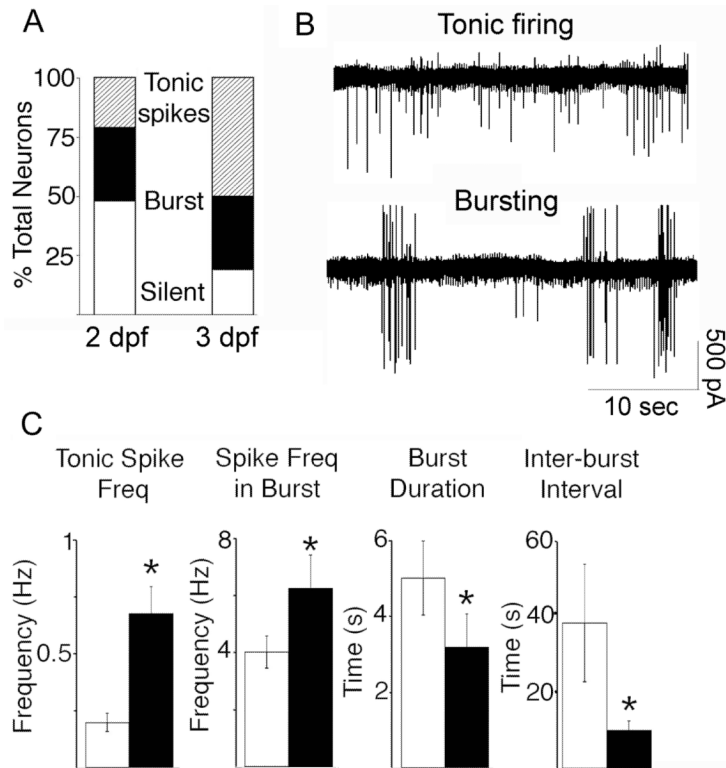
Figure 4.
Loose-patch electrophysiology recordings from 2 dpf (n=29 cells from 17 embryos) and 3 dpf (n=26 cells from 15 embryos) transgenic embryos. *A*: Percent of total TN-GnRH3:EMD neurons that were either electrically silent or showed very few action currents during the period of recording, showed a bursting pattern of action currents, or showed a tonic pattern of action currents. *B*: Representative traces from neurons that showed a tonic or bursting pattern of firing. *C*: Comparison of characteristics of electrical activity between 2 dpf (white bars) and 3 dpf (black bars) embryos (mean ± SEM). From left to right: frequency of tonic firing; frequency of firing within each burst; duration of the bursts; and, inter-burst interval. Asterisks denote statistically significant differences between age groups.